

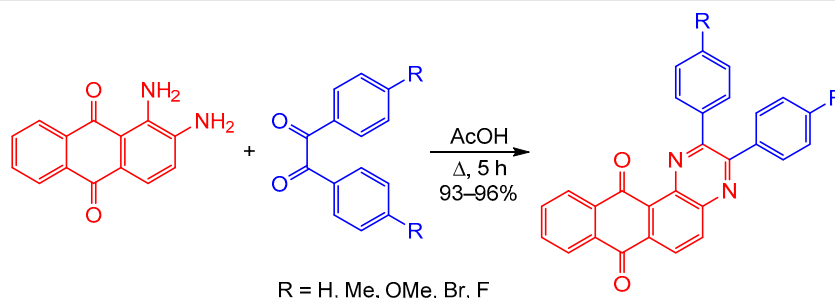
Electron-deficient molecules: photophysical, electrochemical, and thermal investigations of naphtho[2,3-*f*]quinoxaline-7,12-dione derivatives

Azam M. Shaikh¹, Bharat K. Sharma¹, Rajesh M. Kamble^{1*}

¹ Department of Chemistry, University of Mumbai, Santacruz (East), Mumbai-400 098, India; e-mail: kamblerm@chem.mu.ac.in

Published in Khimiya Geterotsiklicheskih Soedinenii, 2016, 52(2), 110–115

Submitted December 28, 2015
Accepted February 8, 2016



In this work, we have prepared a series of 2,3-disubstituted naphtho[2,3-*f*]quinoxaline-7,12-dione derivatives by condensing 1,2-diaminoanthraquinone and various benzil compounds in glacial acetic acid with excellent yield and fully characterized. Optical properties of the synthesized compounds were studied in solvents of varying polarity and thin solid film. Electrochemical properties of the compounds were studied by the cyclic voltammetry. The ionization potentials (HOMO) and electron affinity (LUMO) were found to be in the range of -6.364 to -6.644 eV and -3.247 to -3.511 eV, respectively. Thermal investigations were carried out by thermogravimetric analysis and differential scanning calorimetry.

Keywords: naphtho[2,3-*f*]quinoxaline-7,12-dione, electron acceptor/transporter, fluorescence, HOMO and LUMO energy levels, thermal properties, UV-Vis absorption.

Quinoxaline derivatives are important class of nitrogen-containing heterocyclic compounds and display a wide range of biological properties, such as antiviral,¹ anticancer,^{2,3} antibacterial,⁴ and tyrosine kinase inhibitory.⁵ Apart from biological properties, many quinoxaline derivatives are used as fluorescent derivatization agents⁶ and electroluminescent materials.^{7–9} Molecules with donor–acceptor architecture have been found to exhibit unique charge transfer properties and find applications in the field of organic optoelectronic devices.¹⁰ 2,3-Disubstituted naphtho[2,3-*f*]quinoxaline-7,12-dione derivatives belong to a class of donor–acceptor molecules and can be used in the electroluminescent devices. In literature, a few synthetic routes for the synthesis of 2,3-disubstituted naphtho[2,3-*f*]quinoxaline-7,12-diones **1** and **2** by the condensation of 1,2-diaminoanthraquinone with various benzil derivatives have been reported using propylsulfonic acid functionalized nanozeolite clinoptilolite (Nano CP) as heterogeneous catalyst,¹¹ or reusable polyaniline sulfate salt catalyst.^{12,13} However compounds **3–5** are not reported in the literature. To the best of our knowledge, the opto-

electronic and thermal properties of 2,3-disubstituted naphtho[2,3-*f*]quinoxaline-7,12-dione are not yet studied. Thus, considering the importance of naphtho[2,3-*f*]quinoxaline-7,12-dione moiety, we decided to synthesize a small series of compounds containing it and to study their photophysical, electrochemical, and thermal properties. We further assumed that the optoelectronic properties of 2,3-diphenylnaphtho[2,3-*f*]quinoxaline-7,12-diones can be tuned by introducing into the *para* position of the phenyl ring of electron-donating (Me, OMe) and electron-withdrawing (Br, F) substituents.

2,3-Diarylnaphtho[2,3-*f*]quinoxaline-7,12-diones **1–5** were synthesized by condensation of 1,2-diaminoanthraquinone (**6**) with substituted benzils **7** in glacial acetic acid (Scheme 1). The identity and purity of compounds **1–5** were confirmed by FT-IR, ¹H, ¹³C NMR spectroscopy, mass spectrometry, and elemental analysis. A doublet for each hydrogen at positions 5 and 6 and characteristic signals for two carbonyl groups at positions 7 and 12 were observed in ¹H and ¹³C NMR spectra, respectively, in all compounds **1–5**.

Scheme 1

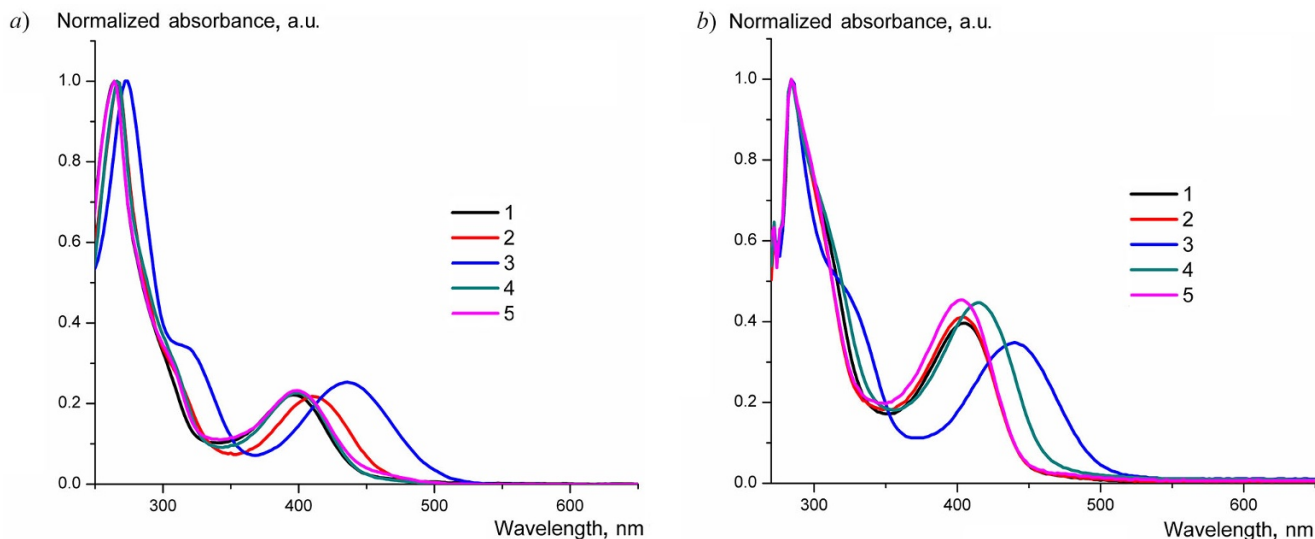
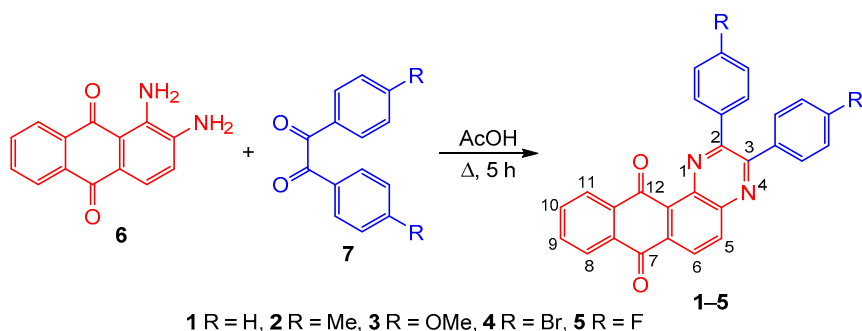


Figure 1. Normalized UV-Vis absorption spectrum of compounds 1–5 in a) dichloromethane, b) toluene.

The photophysical properties of compounds 1–5 were tested in solvents of varying polarity (*n*-hexane, toluene, dichloromethane, chloroform, and tetrahydrofuran), and thin solid film, in order to study the effect of solvent polarity. The synthesized compounds 1–5 show similar UV-Vis absorption spectra in all above solvents and thin solid film (Fig. 1). The UV-Vis absorption spectra of compounds 1–5 show major bands with maxima at 262–282 nm corresponding to $n-\pi^*$, $\pi-\pi^*$ transitions (Table 1).

Apart from $n-\pi^*$, $\pi-\pi^*$ transitions, compounds 1–5 also show a lower energy transition at 396–442 nm that could be attributed to the charge transfer from the electron-donating quinoxaline moiety to the electron-deficient

carbonyl groups. However, quinoxaline moiety itself is electron-deficient due to the presence of imine group, but in the presence of more electron-withdrawing carbonyl group it acts as electron donor. In compound 3, bathochromic shift of charge transfer transition band in a range of 36–40 nm with respect to that of its unsubstituted analog 1 was observed due to the presence of the electron-donating OMe group at the *para* position of the phenyl ring.

Upon irradiation at 350 nm, compounds 1–5 showed emission in the blue region with emission maxima at 402–414 and 426–438 nm (Fig. 2). The emission bands of compounds 1–5 in the blue region could be attributed to the charge transfer interaction in the naphtho[2,3-*f*]quinoxaline-

Table 1. UV-Vis absorption maxima wavelengths and extinction coefficients of compounds 1–5

Compound	λ_{abs} , nm ($\log \epsilon_{\text{max}}$, $\text{M}^{-1} \times \text{cm}^{-1}$)*					Film
	<i>n</i> -Hexane	Toluene	CH_2Cl_2	CHCl_3	THF	
1	262 (5.11), 396 (4.33)	284 (4.66), 404 (4.32)	264 (5.20), 396 (4.54)	266 (5.37), 402 (4.54)	262 (5.00), 396 (4.41)	285, 422
2	266 (5.20), 410 (4.57)	284 (4.86), 414 (4.51)	266 (5.04), 410 (4.38)	268 (5.12), 418 (4.51)	263 (5.12), 380 (4.34)	280, 428
3	274 (5.13), 432 (4.53)	284 (4.72), 440 (4.26)	274 (5.12), 436 (4.52)	274 (5.09), 442 (4.48)	272 (5.02), 434 (4.49)	274, 446
4	266 (4.55), 398 (3.84)	284 (4.89), 406 (4.48)	266 (5.19), 400 (4.55)	268 (5.28), 402 (4.65)	260 (5.38), 402 (4.54)	277, 415
5	264 (4.77), 400 (4.06)	284 (4.68), 404 (4.29)	264 (5.20), 396 (4.56)	266 (5.20), 404 (4.58)	266 (5.18), 396 (4.48)	275, 415

* Recorded in 10^{-5} M solution.

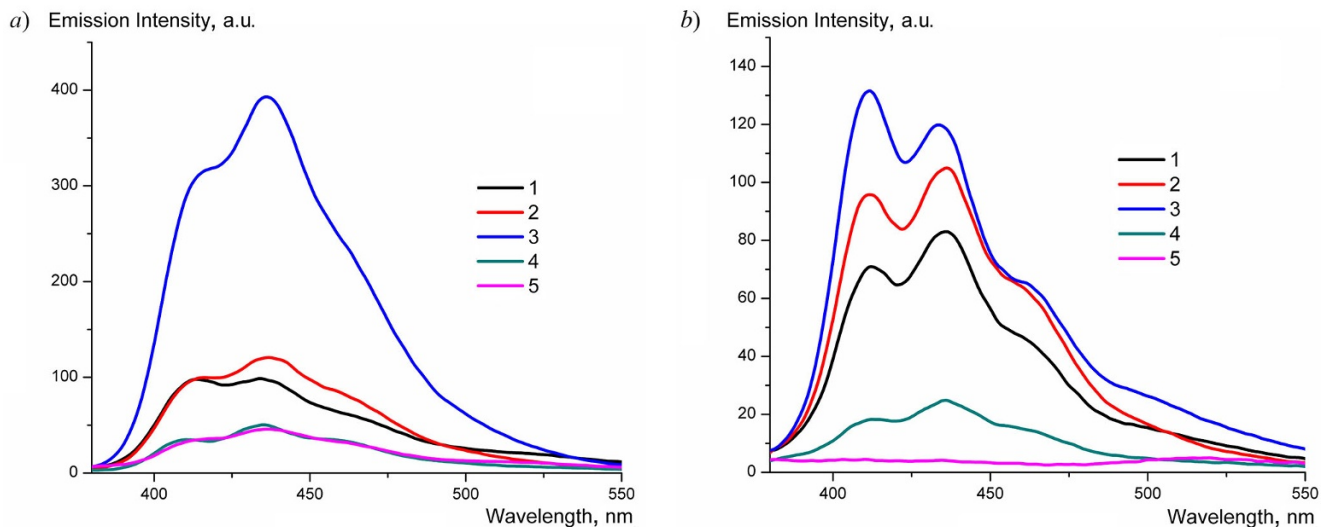


Figure 2. Emission spectra of compounds **1–5** excited at λ 350 nm in a) dichloromethane, b) toluene. (Normed to the $\log \epsilon$ values of the absorption at the excitation wavelength).

7,12-dione backbone between the electron-donating quinoxaline moiety and electron-accepting carbonyl groups.¹⁴ Other basic photophysical characteristics, such as the molar extinction coefficient ($\log \epsilon$), optical band gap (E_g^{opt}), Stokes shift ($\nu_{\text{abs}} - \nu_{\text{em}}$), and fluorescence quantum yield (Φ_F) of the molecules also were determined, and the pertinent data are summarized in Tables 1 and 2.

Optical band gap energy was calculated from the intersection of normalized excitation and emission spectra.^{15,16} The fluorescence quantum yields (Φ_F) were calculated relative to 9,10-diphenylanthracene in cyclohexane ($\Phi_{\text{ref}} = 0.90$ in 10^{-5} M cyclohexane solution) as a reference for blue emitting materials using standard equation (1).¹⁴

$$\Phi_F = \Phi_{\text{ref}} \left(\frac{S_{\text{sample}}}{S_{\text{ref}}} \right) \left(\frac{A_{\text{ref}}}{A_{\text{sample}}} \right) \left(\frac{\eta_{\text{sample}}^2}{\eta_{\text{ref}}^2} \right), \quad (1)$$

where S_{ref} , A_{ref} , η_{ref} and S_{sample} , A_{sample} , η_{sample} represent the integrated emission band area, the absorbance at the excitation wavelength, and the refractive index of the solvent, respectively, for the standard reference and the sample. The Stokes shifts (cm^{-1}) were determined by equation (2):¹⁴

$$(\nu_{\text{abs}} - \nu_{\text{em}}) = \left(\frac{1}{\lambda_{\text{abs}}} - \frac{1}{\lambda_{\text{em}}} \right) \times 10^7. \quad (2)$$

The ionization potential (E_{HOMO}) and electron affinity (E_{LUMO}) of compounds **1–5** were determined by cyclic voltammetry (CV) (Fig. 3) in anhydrous dichloromethane solution using ferrocene as an internal standard to calibrate the redox potentials. The pertinent data are presented in Table 3. On anodic sweep (forward scan) no peaks were observed, except in the case of compound **3**. One irreversible wave was observed in the solution of compound **3** corresponding to oxidation of the methoxy group (Fig. 3b). On cathodic sweep (backward scan) two reversible waves were observed for all compounds **1–5** corresponding to the reduction of two carbonyl groups (Fig. 3a).

The HOMO energy values of compounds **1–5** were calculated from the difference of optical band gap and LUMO energy level (equation (3)) whereas LUMO energy was calculated from the first reduction potential (equation (4)).¹⁷

$$E_{\text{HOMO}} = -(E_g^{\text{opt}} - E_{\text{LUMO}}) \quad (3)$$

$$E_{\text{LUMO}} = -(E_{\text{red}}^{\text{peak}} - E_{\text{red}}(\text{Fc}/\text{Fc}^+) + 4.8) \quad (4)$$

The HOMO and LUMO energy levels of compounds **1–5** are in the range of -6.364 to -6.644 eV and -3.247 to -3.511 eV, respectively (Table 3). Furthermore, the LUMO energy levels of these molecules are comparable to those

Table 2. Emission maximum wavelength, Stokes shift, optical band gap, and quantum yield values of compounds **1–5**

Compound	$\lambda_{\text{em}},^* \text{ nm}$				$\nu_{\text{abs}} - \nu_{\text{em}},^{**} \text{ cm}^{-1}$	$E_g^{\text{opt}},^{**} \text{ eV}$	Φ_F^{**}
	CH_2Cl_2	CHCl_3	Toluene	Film			
1	414, 437	410, 437	413, 436	412, 434	14710	3.14	0.07
2	413, 436	414, 436	411, 436	413, 436	14943	3.13	0.10
3	413, 436	411, 433	411, 435	417, 445	13560	3.12	0.20
4	414, 436	413, 435	411, 435	413, 433	14658	3.14	0.05
5	414, 436	414, 436		414, 438	14943	3.15	0.06

* Recorded in 10^{-5} M solution.

** Calculated from the data recorded in 10^{-5} M CH_2Cl_2 solution.

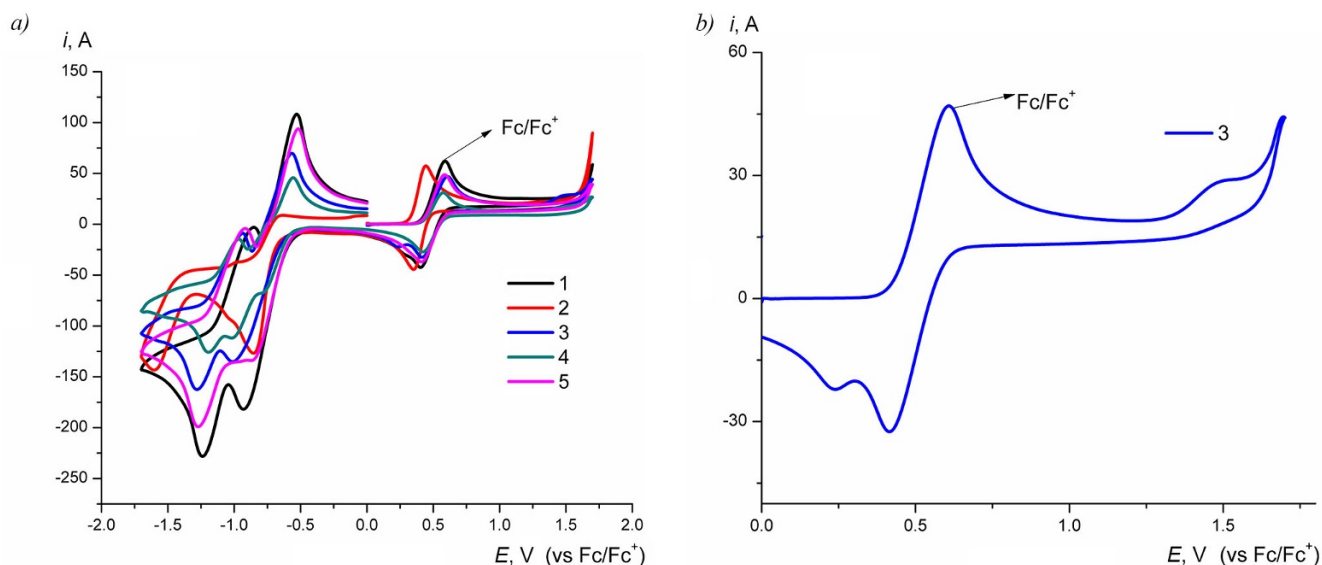


Figure 3. a) Cyclic voltammogram (full scan) of compounds **1–5** in 10^{-3} M CH_2Cl_2 solution with ferrocene as reference. b) Cyclic voltammogram of compound **3** (anodic sweep).

reported for electron-transporting/injecting polyquinoxalines.^{18–21} Therefore, compounds **1–5** may act as electron-transporting/injecting materials.

The thermal stability of compounds **1–5** was determined using thermogravimetric analysis (TGA) (Fig. 4a). Melting points of compounds **1–5** were determined by differential scanning calorimetry (DSC) and are in the range of 235–301°C (Fig. 4b). TGA thermogram (Fig. 4a) reveals that compounds **1–5** have good thermal stability with no weight loss at low temperature. The decomposition temperature values corresponding to 5 and 10% weight loss were in the range of 280–365 and 325–430°C, respectively (Table 3).

The order of thermal stability among compounds **1–5** is **4** > **2** > **3** > **5** > **1**. No glass transition temperature was observed. In the derivative weight loss plot (see Supplementary information), compounds **1**, **4**, and **5** show single step decomposition, whereas compounds **2** and **3** show three decomposition steps.

Table 3. Electrochemical and thermal data of compounds **1–5**

Compound	$E_{\text{ox}}^{\text{peak}}$, V	$E_{\text{red}}^{\text{peak}}$, V	E_{HOMO} , eV	E_{LUMO} , eV	T_m , *** °C	T_d , ** ⁴ °C
1		−0.886, −1.242	−6.444	−3.327	282	280 (325)
2		−0.846, −1.569	−6.644	−3.511	278	360 (430)
3	1.489	−0.930, −1.286	−6.396	−3.263	235	355 (390)
4		−0.982, −1.258	−6.364	−3.247	301	365 (380)
5		−0.930, −1.286	−6.487	−3.362	291	330 (355)

* Oxidation peak potential.

** Reduction peak potential.

*** Melting point determined by DSC.

**⁴ Decomposition temperature at 5 and 10% (in parentheses) weight loss derived by TGA.

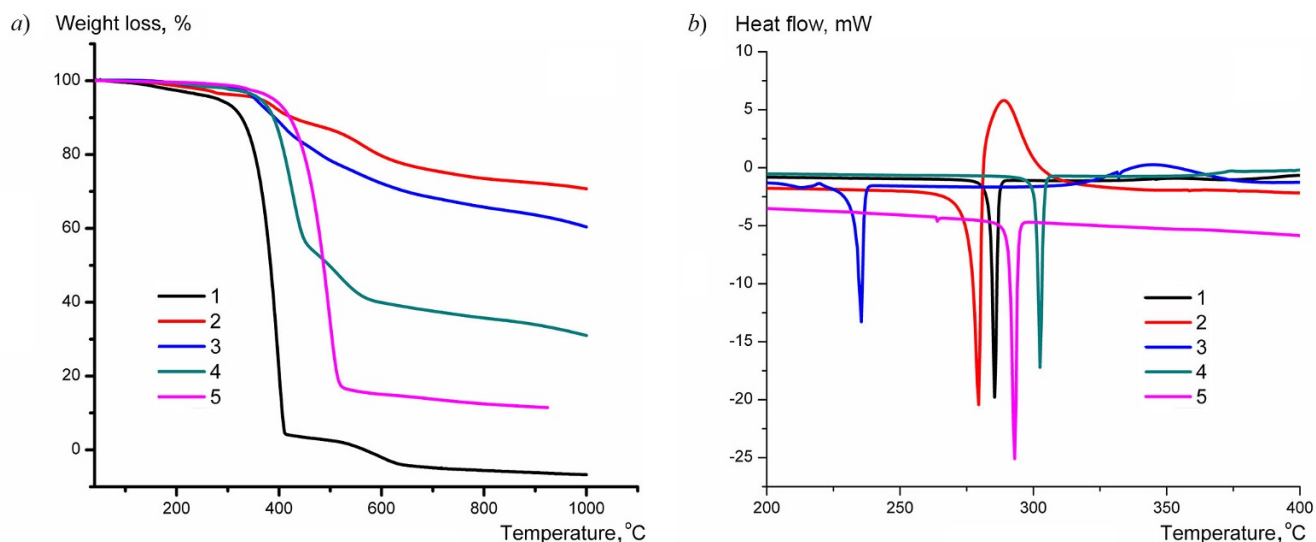


Figure 4. a) TGA thermogram and b) DSC plot of compounds **1–5**.

In conclusion, we have prepared a series of donor–acceptor type 2,3-disubstituted naphtho[2,3-*f*]quinoxaline-7,12-dione derivatives with excellent yield. The absorption spectra of all studied compounds show the presence of intramolecular charge transfer transition bands. The electron affinities (LUMO energy levels) of the synthesized compounds are comparable to those of electron-transporting/injecting materials reported in literature. The investigated compounds have high melting points and good thermal stability. Therefore, these compounds are potential candidates for electron-transporting/injecting applications in organic electronics.

Experimental

UV-Vis spectra were recorded on a Shimadzu UV-2401 PC spectrophotometer at room temperature in 10^{-5} M solution (quartz cuvette, path length 1 cm) or in thermally deposited thin solid film. The fluorescence emission spectra were recorded on a Perkin Elmer LS 55 spectrofluorimeter. Fourier-transform IR spectra were recorded on a Perkin Elmer Frontier 91579 instrument in KBr. ^1H and ^{13}C NMR spectra were recorded on a Bruker 300 Ultrashield spectrometer (300 and 75 MHz, respectively) in CDCl_3 with TMS as internal standard. Mass spectra were recorded on a Thermo Scientific Polaris Q GC-MS instrument. Elemental analysis was carried out on a Euro EA 3000 elemental analyzer. Melting points were determined by DSC. TGA and DSC experiments were performed on a Metler–Toledo instrument under nitrogen atmosphere. Column chromatography was carried out using SD–Fine silica gel (60–120 mesh), eluting with *n*-hexane and chloroform. Cyclic voltammetry studies were carried out on a computer-controlled PalmSens3 potentiostat/galvanostat. Typically, a three-electrode cell, equipped with a glassy carbon working electrode, Ag/AgCl (non-aqueous) reference electrode, and Pt wire as counter electrode, was employed. The measurements have been carried at room temperature in anhydrous dichloromethane (10^{-3} M) with Bu_4NPF_6 (0.1 M) as supporting electrolyte and a scan rate $100 \text{ mV} \times \text{s}^{-1}$. The potential of Ag/AgCl reference electrode was calibrated by using ferrocene/ferrocenium redox couple which has the known oxidation potential of +4.8 eV.^{9,22}

The progress of reactions and the purity of the products were checked by TLC on silica gel-coated glass plates. The spots were visualized with UV light and in iodine chamber.

Preparation of 2,3-diarylnaphtho[2,3-*f*]quinoxaline-7,12-diones 1–5 (General method). A mixture of benzil derivative **7** (1.0 mmol) and 1,2-diaminoanthraquinone (**6**) (0.238 g, 1 mmol) was dissolved in glacial acetic acid (20 ml) and refluxed for 5 h. The reaction mixture was allowed to cool and then poured onto crushed ice to obtain the orange to red colored solid which was dried under vacuum and purified using column chromatography (eluent *n*-hexane– CHCl_3 , 3:2) to obtain a bright-orange to red solid.

2,3-Diphenylnaphtho[2,3-*f*]quinoxaline-7,12-dione (1). Yield 93%, orange solid, mp 282°C (mp $272\text{--}275^\circ\text{C}^{11}$). IR spectrum, ν , cm^{-1} : 3083, 2921, 2851, 1651, 1581, 1265. ^1H NMR spectrum, δ , ppm (*J*, Hz): 8.64 (1H, d, *J* = 9.0,

H-6); 8.46 (1H, d, *J* = 9.0, H-5); 8.28–8.35 (2H, m, H Ar); 7.79–7.84 (4H, m, H Ar); 7.68–7.70 (2H, m, H Ar); 7.37–7.67 (6H, m, H Ar). ^{13}C NMR spectrum, δ , ppm: 183.5 (C=O); 183.4 (C=O); 155.2; 154.3; 143.0; 138.3; 138.1; 135.1 (2C); 134.5; 133.5; 132.2; 130.4; 129.8 (2C); 129.7; 128.5 (2C); 127.3; 126.7; 126.6. Mass spectrum, *m/z* (I_{rel} , %): 411 (100), 412 $[\text{M}]^+$ (85). Found, %: C 81.50; H 3.93; N 6.80; O 7.77. $\text{C}_{28}\text{H}_{16}\text{N}_2\text{O}_2$. Calculated, %: C 81.54; H 3.91; N 6.79; O 7.76.

2,3-Bis(4-methylphenyl)naphtho[2,3-*f*]quinoxaline-7,12-dione (2). Yield 95%, orange solid, mp 278°C (mp $263\text{--}265^\circ\text{C}^{12}$). IR spectrum, ν , cm^{-1} : 3082, 2926, 2852, 1666, 1587, 1265. ^1H NMR spectrum, δ , ppm (*J*, Hz): 8.58 (1H, d, *J* = 9.0, H-6); 8.41 (1H, d, *J* = 9.0, H-5); 8.26–8.33 (2H, m, H Ar); 7.71–7.82 (4H, m, H Ar); 7.59 (2H, d, *J* = 9.0, H Ar); 7.19 (4H, d, *J* = 9.0, H Ar); 2.40 (6H, s, CH_3). ^{13}C NMR spectrum, δ , ppm: 183.5 (C=O); 183.4 (C=O); 155.1; 154.2; 142.9; 139.9; 138.4; 137.9; 135.6; 135.4; 135.2 (2C); 134.9; 134.4; 133.4; 132.2; 130.3; 129.7; 129.3; 129.2 (2C); 127.3; 126.6; 126.3; 21.4 (CH_3). Mass spectrum, *m/z* (I_{rel} , %): 440 $[\text{M}]^+$ (80), 425 $[\text{M}-\text{CH}_3]^+$ (100). Found, %: C 81.78; H 4.60; N 6.34; O 7.27. $\text{C}_{30}\text{H}_{20}\text{N}_2\text{O}_2$. Calculated, %: C 81.80; H 4.58; N 6.36; O 7.26.

2,3-Bis(4-methoxyphenyl)naphtho[2,3-*f*]quinoxaline-7,12-dione (3). Yield 96%, red solid, mp 235°C . IR spectrum, ν , cm^{-1} : 3065, 2926, 1659, 1602, 1513, 1286, 1248. ^1H NMR spectrum, δ , ppm (*J*, Hz): 8.56 (1H, d, *J* = 9.0, H-6); 8.36 (1H, d, *J* = 9.0, H-5); 8.26–8.33 (2H, m, H Ar); 7.66–7.83 (6H, m, H Ar); 6.90–6.94 (4H, m, H Ar); 3.85 (6H, s, OCH_3). ^{13}C NMR spectrum, δ , ppm: 183.6 (C=O); 183.4 (C=O); 161.0; 154.5; 153.6; 142.8; 138.4; 135.1; 134.9; 134.8; 134.4; 133.4; 132.2; 131.9; 131.3; 131.0; 130.6; 129.2; 127.2; 126.6; 126.1; 55.3 (OCH_3). Mass spectrum, *m/z* (I_{rel} , %): 472 $[\text{M}]^+$ (100), 441 $[\text{M}-\text{OCH}_3]^+$ (70). Found, %: C 76.30; H 4.20; N 5.95; O 13.58. $\text{C}_{30}\text{H}_{20}\text{N}_2\text{O}_4$. Calculated, %: C 76.26; H 4.27; N 5.93; O 13.54.

2,3-Bis(4-bromophenyl)naphtho[2,3-*f*]quinoxaline-7,12-dione (4). Yield 93%, orange solid, mp 302°C . IR spectrum, ν , cm^{-1} : 3069, 2920, 1665, 1582, 1328. ^1H NMR spectrum, δ , ppm (*J*, Hz): 8.66 (1H, d, *J* = 9.0, H-6); 8.45 (1H, d, *J* = 9.0, H-5); 8.29–8.35 (2H, m, H Ar); 7.78–7.88 (2H, m, H Ar); 7.67–7.71 (2H, m, H Ar); 7.54–7.58 (6H, m, H Ar). ^{13}C NMR spectrum, δ , ppm: 183.3 (C=O); 183.2 (C=O); 153.7; 152.8; 142.9; 137.0; 136.6; 135.7; 135.0; 134.6; 133.6; 132.1; 132.0; 131.8; 131.3; 127.3; 127.0; 126.7; 124.8. Mass spectrum, *m/z* (I_{rel} , %): 570 $[\text{M}]^+$ (98), 491 $[\text{M}-\text{Br}]^+$ (100). Found, %: C 58.80; H 2.49; Br 28.05; N 4.92; O 5.58. $\text{C}_{28}\text{H}_{14}\text{Br}_2\text{N}_2\text{O}_2$. Calculated, %: C 58.98; H 2.47; Br 28.03; N 4.91; O 5.61.

2,3-Bis(4-fluorophenyl)naphtho[2,3-*f*]quinoxaline-7,12-dione (5). Yield 94%, orange solid, mp 291°C . IR spectrum, ν , cm^{-1} : 3070, 2921, 1667, 1591, 1504, 1220. ^1H NMR spectrum, δ , ppm (*J*, Hz): 8.65 (1H, d, *J* = 9.0, H-6); 8.44 (1H, d, *J* = 9.0, H-5); 8.29–8.35 (2H, m, H Ar); 7.78–7.88 (4H, m, H Ar); 7.67–7.70 (2H, m, H Ar); 7.08–7.15 (4H, m, H Ar). ^{13}C NMR spectrum, δ , ppm: 183.5 (C=O); 183.3 (C=O); 153.8; 152.9; 142.9; 138.5; 135.5; 135.0; 134.6; 133.3; 132.5; 132.3; 132.1; 131.9; 131.8;

129.3; 127.3; 126.9; 126.7; 116.0; 115.9; 115.7 (2C). Mass spectrum, m/z (I_{rel} , %): 448 $[M]^+$ (100), 391 (25). Found, %: C 75.03; H 3.16; F 8.45; N 6.23; O 7.13. $C_{28}H_{14}F_2N_2O_2$. Calculated, %: C 75.00; H 3.15; F 8.47; N 6.25; O 7.14.

Supplementary information file to this article containing IR, 1H and ^{13}C NMR, and mass spectra, complete photophysical data, and derivative weight loss plot of compounds 1–5 is available at <http://link.springer.com/journal/10593>.

References

- Lindsley, C. W.; Zhao, Z.; Leister, W. H.; Robinson, R. G.; Barnett, S. F.; Defeo-Jones, D.; Jones, R. E.; Hartman, G. D.; Huff, J. R.; Huber, H. E.; Duggan, M. E. *Bioorg. Med. Chem. Lett.* **2005**, *15*, 761.
- Loriga, M.; Piras, S.; Sanna, P.; Paglietti, G. *Farmaco* **1997**, *52*, 157.
- Kim, Y. B.; Kim, Y. H.; Park, J. Y.; Kim, S. K. *Bioorg. Med. Chem. Lett.* **2004**, *14*, 541.
- Seitz, L. E.; Suling, W. J.; Reynolds, R. C. *J. Med. Chem.* **2002**, *45*, 5604.
- He, W.; Myers, M. R.; Hanney, B.; Spada, A. P.; Bilder, G.; Galzinski, H.; Amin, D.; Needle, S.; Page, K.; Jayyosi, Z.; Perrone, M. H. *Bioorg. Med. Chem. Lett.* **2003**, *13*, 3097.
- Katoh, A.; Yoshida, T.; Ohkanda, J. *Heterocycles* **2000**, *52*, 911.
- Thomas, K. R. J.; Velusamy, M.; Lin, J. T.; Chuen, C. H.; Tao, Y. T. *Chem. Mater.* **2005**, *17*, 1860.
- Shaikh, A. M.; Sharma, B. K.; Kamble, R. M. *J. Chem. Sci.* **2015**, *127*, 1571.
- Shaikh, A. M.; Sharma, B. K.; Kamble, R. M. *Can. Chem. Trans.* **2015**, *3*, 158.
- Shirota, Y. *J. J. Mat. Chem.* **2000**, *10*, 1.
- Baghbanian, S. M. *Chin. Chem. Lett.* **2015**, *26*, 1113.
- Srinivas, Ch.; Kumar, Ch. N. S. S. P.; Rao, V. J.; Palaniappan. S. *Catal. Lett.* **2008**, *121*, 291.
- Srinivas, Ch.; Kumar, Ch. N. S. S. P.; Rao, V. J.; Palaniappan. S. *J. Mol. Catal. A: Chem.* **2007**, *265*, 227.
- Ulla, H.; Garudachari, B.; Satyanarayan, M. N.; Umesh, G.; Isloor, A. M. *Opt. Mater. (Amsterdam, Neth.)* **2014**, *36*, 704.
- Agarwal, N.; Nayak, P. K.; Ali, F.; Patankar, M. P.; Narasimhan, K. L.; Periasamy, N. *Synth. Met.* **2011**, *161*, 466.
- Sharma, B. K.; Shaikh, A. M.; Agarwal, N.; Kamble, R. M. *RSC Adv.* **2016**, *6*, 17129.
- Kamble, R. M.; Shaikh, A. M.; Sharma, B. K. *Chem. Sci. Trans.* **2015**, *4*, 781.
- Kulkarni, A. P.; Tonzola, C. J.; Babel, A.; Jenekhe, S. A. *Chem. Mater.* **2004**, *16*, 4556.
- Fukuda, T.; Kanbara, T.; Yamamoto, T.; Ishikawa, K.; Takezoe, H.; Fukuda, A. *Appl. Phys. Lett.* **1996**, *68*, 2346.
- O'Brien, D.; Weaver, M. S.; Lidzey, D. G.; Bradley, D. D. C. *Appl. Phys. Lett.* **1996**, *69*, 881.
- Cui, Y.; Zhang, X.; Jenekhe, S. *Macromolecules* **1999**, *32*, 3824.
- Sharma, B. K.; Shaikh, A. M.; Kamble, R. M. *J. Chem. Sci.* **2015**, *127*, 2063.